What does the muon spin-relaxation rate measure in 4f paramagnets with strong crystal fields and weak inter-site correlations?

1996 J. Phys.: Condens. Matter 8 5113

(http://iopscience.iop.org/0953-8984/8/27/020)

J. Phys.: Condens. Matter **8** (1996) 5113–5123. Printed in the UK

What does the muon spin-relaxation rate measure in 4f paramagnets with strong crystal fields and weak inter-site correlations?

P Dalmas de Réotier†, A Yaouanc† and P Bonville‡

† Commissariat à l'Energie Atomique, Département de Recherche Fondamentale sur la Matière Condensée, F-38054 Grenoble Cédex 9, France

‡ Commissariat à l'Energie Atomique, Département de Recherches sur l'Etat Condensé, les Atomes et les Molécules, F-91191 Gif-sur-Yvette, France

Received 19 February 1996, in final form 15 April 1996

Abstract. We investigate the physical meaning of the longitudinal muon spin-relaxation rate λ_Z measured for a paramagnet at temperatures high with respect to the magnetic phase transition temperature. The depolarization rate λ_Z is shown to be a function of the relaxation rates of the quasi-elastic and inelastic magnetic excitations. Using this analysis, we consider recently published μSR data recorded on the strongly correlated electron systems CeNiSn and $CePt_2Sn_2$.

1. Introduction

Positive muon spectroscopy (μSR) has been intensively used to probe the static magnetic properties of magnets at the microscopic level, in particular in the strongly correlated compounds [1]. The dynamical magnetic properties of these compounds in the paramagnetic phase have not been much studied, notwithstanding the fact that magnetic ordering, if any, generally occurs at very low temperature. The absence of a detailed theoretical framework for the analysis of μSR data recorded far into the paramagnetic state, especially when a sizeable crystal-electric-field (CEF) interaction is present, may however explain this lack of interest. The purpose of this paper is to provide such a framework and to give examples of its use by analysing recently published μSR data in the strongly correlated electron systems CeNiSn and $CePt_2Sn_2$. In a separate work we use this framework to analyse μSR data in the Yb-based weak Kondo lattice $YbAuCu_4$ [2].

The organization of this paper is as follows. In section 2 we derive the relation between the longitudinal μSR relaxation rate λ_Z and the spin–spin correlation functions of the paramagnet. We neglect the inter-site correlations and assume that the motional narrowing approximation is valid. In section 3, λ_Z is expressed in terms of the spectral functions of magnetic excitations. Our approach should be particularly useful for the description of compounds with f-electronic-shell ions. In section 4 we analyse published μSR data recorded for CeNiSn and $CePt_2Sn_2$. In section 5 we summarize our work. Some useful matrix elements are listed in an appendix.

2. The longitudinal μSR relaxation rate and spin–spin correlation functions

In the μSR technique [3, 4] polarized muons are implanted into a sample where their spin evolves in the local magnetic field until they decay. The decay positron is emitted

0953-8984/96/275113+11$19.50

preferentially along the final muon spin direction; by collecting several million positrons, we can reconstruct the time dependence of the muon spin-depolarization function $P_Z(t)$ which, in turn, reflects the evolution of the field at the muon site. The Z-axis refers to the muon beam polarization axis which, in our case, is the direction of the detected positrons. This longitudinal geometry is best suited for the study of spin dynamics.

We suppose that the μSR spectra are not influenced by the nuclear magnetic moments of the compound under study. This means that they are eventually recorded in a weak magnetic field applied along the Z-axis. This field, which is typically about 10 mT, is sufficiently low that it does not influence the spin dynamics and the relationship between λ_Z and the spin–spin correlation functions. Basically to give a numerical value, experiments performed in a 10 mT longitudinal field probe the dynamical susceptibility at an energy of 5.6 neV which we take as 0.

We assume that the motional narrowing approximation is valid. This means that we only consider compounds characterized by relatively fast dynamics. This is usually the case. An example of the breakdown of the motional narrowing approximation at low temperature is given in [5].

Within this hypothesis $P_Z(t)$ is an exponential function characterized by a relaxation rate λ_Z which can be expressed in terms of the field correlation functions at the muon site [6]. Previously these functions were written in the laboratory reference frame $(\boldsymbol{X}, \boldsymbol{Y}, \boldsymbol{Z})$ where $\boldsymbol{X}$, $\boldsymbol{Y}$, and $\boldsymbol{Z}$ are unit vectors. But the magnetic properties of the compound are more easily described in an orthogonal reference frame $(\boldsymbol{x}, \boldsymbol{y}, \boldsymbol{z})$ attached to the crystal axes rather than to the laboratory. Its unit vectors are chosen parallel to the crystal axes according to the symmetry of the compound.

As can be seen from the definition of the μSR depolarization function, the Z-axis is of special importance. We define $\boldsymbol{Z}$ in the $(\boldsymbol{x}, \boldsymbol{y}, \boldsymbol{z})$ frame by its polar angles θ and φ. With these angles the expression for the μSR relaxation rate in terms of the correlation tensor in the crystal axes is

$$\lambda_Z = \pi \gamma_\mu^2 \sum_{\beta,\alpha} L_{\beta\alpha}(\theta, \varphi) \tilde{\Phi}_{\alpha\beta} \tag{1}$$

where $L(\theta, \varphi)$ is a matrix, the elements of which are given in appendix A, and $\tilde{\Phi}$ is a field correlation function at zero energy transfer written in the $(\boldsymbol{x}, \boldsymbol{y}, \boldsymbol{z})$ reference frame, with $\{\alpha, \beta\} = \{x, y, z\}$.

The tensor $\tilde{\Phi}_{\alpha\beta}$ can be expressed as a sum over crystal sites of a product of the symmetrized correlation tensor $\tilde{\Lambda}$ of the total angular momenta of the magnetic ions, and of tensors $\tilde{G}$ describing the coupling between the muon spin and the total angular momenta [6, 7]:

$$\tilde{\Phi}_{\alpha\beta} = \left(\frac{\mu_0}{4\pi}\right)^2 \left(g_J \mu_B\right)^2 \frac{1}{v^2} \sum_{\gamma,\gamma'} \sum_{i,d} \sum_{i',d'} G^{\alpha\gamma}_{\boldsymbol{r}_{i+d}} G^{\gamma'\beta}_{\boldsymbol{r}_{i'+d'}} \tilde{\Lambda}^{\gamma\gamma'}_{ii',dd'} \tag{2a}$$

with

$$G^{\alpha\gamma}_{\boldsymbol{r}_{i+d}} = v\left(\frac{3 r_{i+d,\alpha} r_{i+d,\gamma}}{r^5_{i+d}} - \frac{\delta^{\alpha\gamma}}{r^3_{i+d}}\right) + H_{r_{i+d}} \delta^{\alpha\gamma}. \tag{2b}$$

In these expressions, μ_0 is the permeability of free space, g_J the spectroscopic Landé factor of the rare earth, and v the volume of the lattice cell used to describe the crystal. The tensor $G_{\boldsymbol{r}_{i+d}}$ describes the coupling between the muon spin and the total angular momentum $\boldsymbol{J}_{i,d}$ of the ion located at the distance $\boldsymbol{r}_{i+d}$ from the muon site, $\boldsymbol{r}_{i+d}$ being a vector which points to site i of sublattice d. In the case of the Bravais lattice the sums over d and d'

reduce to a single term. The quantity $H_{r_{i+d}}$ is the hyperfine tensor which for simplicity we suppose isotropic. The tensor $\tilde{\Lambda}_{ii',dd'}$ is the Fourier transform at zero energy transfer of the spin–spin correlation tensor between total angular momenta $\boldsymbol{J}_{i,d}$ and $\boldsymbol{J}_{i',d'}$.

At this stage, we make the important approximation that the correlations between magnetic moments at different sites are negligible, i.e. we neglect any $\boldsymbol{q}$-dependence of the spin–spin correlation tensors. This approximation is valid at sufficiently high temperature relative to the magnetic phase transition temperature. Therefore we set $\tilde{\Lambda}^{\gamma\gamma'}_{ii',dd'} = \tilde{\Lambda}^{\gamma\gamma'}\delta_{ii'}\delta_{dd'}$. Then we derive

$$\tilde{\Phi}_{\alpha\beta} = \left(\frac{\mu_0}{4\pi}\right)^2 (g_J\mu_B)^2 \sum_{\gamma,\gamma'} \tilde{\Lambda}^{\gamma\gamma'} \frac{1}{v^2} \sum_{i,d} G^{\alpha\gamma}_{\boldsymbol{r}_{i+d}} G^{\gamma'\beta}_{\boldsymbol{r}_{i+d}}. \tag{3}$$

It is always possible to find a frame in which $\tilde{\Lambda}^{\gamma\gamma'}$ is diagonal. In this frame, it is characterized by only one correlation function for the cubic case and two distinct correlation functions in the axial case. In the axial case one can write

$$\tilde{\Lambda}^{\gamma\gamma'} = \tilde{\Lambda}_{\parallel}\delta^{\gamma z}\delta^{\gamma' z} + \tilde{\Lambda}_{\perp}(\delta^{\gamma\gamma'} - \delta^{\gamma z}\delta^{\gamma' z}). \tag{4}$$

Combining the previous two equations we derive

$$\tilde{\Phi}_{\alpha\beta} = (\frac{\mu_0}{4\pi})^2 (g_J\mu_B)^2 \left[(\tilde{\Lambda}_{\parallel} - \tilde{\Lambda}_{\perp}) \frac{1}{v^2} \sum_{i,d} G^{\alpha z}_{\boldsymbol{r}_{i+d}} G^{z\beta}_{\boldsymbol{r}_{i+d}} + \tilde{\Lambda}_{\perp} \frac{1}{v^2} \sum_{\gamma} \sum_{i,d} G^{\alpha\gamma}_{\boldsymbol{r}_{i+d}} G^{\gamma\beta}_{\boldsymbol{r}_{i+d}} \right] \tag{5}$$

where $\tilde{\Lambda}_{\parallel}$ and $\tilde{\Lambda}_{\perp}$ are respectively the parallel and perpendicular correlation functions. In the cubic case, $\tilde{\Lambda}^{\gamma\gamma'}$ is a scalar tensor, i.e. $\tilde{\Lambda}_{\parallel} = \tilde{\Lambda}_{\perp} \equiv \tilde{\Lambda}$, and λ_Z is proportional to $\tilde{\Lambda}$.

The expression for λ_Z can be rather simple if the symmetry at the muon site is high. For example if $G^{\alpha z}_{\boldsymbol{r}_{i+d}} = 0$ for $\alpha = x$ or y, we find then that while $\lambda_Z(\theta = 0)$ is proportional to $\tilde{\Lambda}_{\perp}$, $\lambda_Z(\theta = \pi/2)$ is a weighted sum of $\tilde{\Lambda}_{\parallel}$ and $\tilde{\Lambda}_{\perp}$. In any case, if the point symmetry at the muon site is known, it is possible to determine the correlation functions by combining measurements performed on a single crystal for different orientations of Z relative to the crystal axes.

3. The longitudinal μSR relaxation rate, susceptibilities and spectral functions

In this section we obtain a physically transparent meaning of λ_Z using the results of section 2, and a phenomenological description for the magnetic excitations. In the first subsection we shall derive some formulae and give a model example in the second subsection.

3.1. Formalism

For simplicity we shall study here the case for which $\tilde{\Lambda}^{\gamma\gamma'}$ is scalar. This describes compounds with magnetic ions located in sites of cubic symmetry. The result derived below has been used to analyse μSR data recorded for the Kondo lattice compound $YbAuCu_4$ [2]. As mentioned in the previous section, in cubic symmetry, $\tilde{\Phi}_{\alpha\beta}$ is proportional to the on-site symmetrized spin correlation function $\tilde{\Lambda}$:

$$\tilde{\Lambda} = \frac{1}{2\pi} \int_{-\infty}^{\infty} \mathrm{d}\tau \ \frac{1}{2} [\langle J_z(\tau) J_z + J_z J_z(\tau) \rangle] \tag{6}$$

which is related to the dynamic susceptibility by the fluctuation-dissipation theorem:

$$\tilde{\Lambda} = \frac{1}{\mu_0 (g_J\mu_B)^2} k_B T \lim_{\omega \to 0} \frac{\chi''[\omega]}{\pi\omega}. \tag{7}$$

In this expression, $\chi''[\omega]$ is the one-sided time Fourier transform of the imaginary part of the dynamical susceptibility [8]. For rare-earth paramagnets, it is important to take into account the splitting of the ground spin–orbit multiplet of the 4f shell by the CEF interaction, which is of the order of 100 K in intermetallic compounds. In these latter compounds, where the dynamics of the rare-earth ion is dominated by the coupling between the total momentum $\boldsymbol{J}$ and the conduction electron spin density, general methods have been developed to compute $\chi''[\omega]$ in the presence of CEF splittings [9, 10, 11]. The dynamical susceptibility has also been computed in the case of a Kondo coupling, both for a degenerate 4f ion using the non-crossing-approximation (NCA) scheme [12] and for an ion in the presence of CEF splittings [13].

In order to understand qualitatively the meaning of the μSR longitudinal relaxation rate in the presence of CEF splittings, it is useful to introduce the approximate model that Holland-Moritz *et al* [14] derived for the computation of inelastic neutron scattering spectra. This will provide us with the possibility of analysing the relationship between the dynamical linewidths and λ_Z. The model considers the CEF excitations as independent and accordingly splits the susceptibility into Curie and Van Vleck terms. The coupling between the elastic and inelastic excitations is considered in more elaborate treatments [9, 10, 11]. The dynamical susceptibility is written as

$$\frac{\chi''[\omega]}{\pi\omega} = \sum_m \chi_C^m P_{mm}(\omega) + \frac{1}{2}\sum_{m\neq n} \chi_{VV}^{nm}\left[1-\exp(-\beta\Delta_{nm})\right] P_{nm}\left(\omega - \frac{\Delta_{nm}}{\hbar}\right) \tag{8}$$

where the sums are over the CEF energy levels. Here

$$\chi_C^m = \frac{\mu_0(g_J\mu_B)^2}{k_BT}\rho_m|\langle m|J_z|m\rangle|^2 \tag{9}$$

is the Curie susceptibility of the mth level and

$$\chi_{VV}^{nm} = \mu_0(g_J\mu_B)^2\rho_m\frac{|\langle n|J_z|m\rangle|^2}{\Delta_{nm}} \tag{10}$$

is the Van Vleck susceptibility for the transition from the state with energy E_m to the state with energy E_n. We have $\Delta_{nm} = E_n - E_m$ and $\rho_m = \exp(-\beta E_m)/Z$ where $\beta = 1/k_BT$ and Z is the partition function. The normalized function $P_{nm}(\omega)$ is the spectral function for the mn-excitation (from state $|m\rangle$ to state $|n\rangle$). We shall assume it has a Lorentzian shape, which allows us to compare the muon and neutron scattering data. Then we set

$$P_{nm}(\omega) = \frac{1}{\pi}\frac{\Gamma_{nm}}{\Gamma_{nm}^2+\omega^2} \tag{11}$$

where $\Gamma_{nm}(T)$ is the dynamical half-width at half-maximum for transition mn. Equation (8) has been used intensively for analysing inelastic neutron scattering data recorded for paramagnets. The first and second terms on its right-hand side describe the elastic and inelastic CEF transitions, respectively. The inelastic term contains both the energy-loss and energy-gain contributions.

Introducing the Curie susceptibility for the free ion:

$$\chi_C = \frac{\mu_0(g_J\mu_B)^2J(J+1)}{3k_BT} \equiv \frac{\mu_0\mu_{\text{eff}}^2}{3k_BT} \tag{12}$$

and defining a new form for the coupling tensor between the 4f ion and the muon spin:

$$M_{\alpha\beta} = \gamma_\mu^2\left(\frac{\mu_0}{4\pi}\right)^2\frac{\mu_{\text{eff}}^2}{3}\frac{1}{v^2}\sum_\gamma\sum_{i,d} G_{\boldsymbol{r}_{i+d}}^{\alpha\gamma}G_{\boldsymbol{r}_{i+d}}^{\gamma\beta} \tag{13}$$

we can write the damping rate λ_Z as

$$\lambda_Z = \left[\sum_{\beta,\alpha} L_{\beta\alpha}(\theta,\varphi) M_{\alpha\beta}\right] \frac{1}{\Gamma_{\mu\mathrm{SR}}}. \tag{14}$$

We have introduced here a new dynamical width $\Gamma_{\mu\mathrm{SR}}$ appropriate for the interpretation of μSR data:

$$\frac{1}{\Gamma_{\mu\mathrm{SR}}} = \frac{\pi}{\chi_C}\left\{\sum_m \chi_C^m P_{mm}(\omega=0) + \frac{1}{2}\sum_{m\neq n}\chi_{VV}^{nm}\left[1-\exp(-\beta\Delta_{nm})\right] P_{nm}\left(\frac{\Delta_{nm}}{\hbar}\right)\right\}. \tag{15}$$

Explicitly, we have $P_{mm}(0) = 1/(\pi\Gamma_m)$ and

$$P_{nm}\left(\frac{\Delta_{nm}}{\hbar}\right) = \frac{1}{\pi\Gamma_{nm}}\frac{1}{1+(\Delta_{nm}/\hbar\Gamma_{nm})^2}. \tag{16}$$

It is clear that $\Gamma_{\mu\mathrm{SR}}$ depends on both the elastic and inelastic dynamical linewidths, which have to be computed in each case according to the dominant relaxation mechanism of the 4f ions. We note that if the z- and Z-axes are taken to be parallel, in cubic symmetry we have $M_{xx} = M_{yy} \equiv \Delta_e^2$. It follows that equation (14) can be simply written as

$$\lambda_Z(T) = 2\Delta_e^2\tau(T) \tag{17}$$

where we have defined $\tau = 1/\Gamma_{\mu\mathrm{SR}}$. We recover the well known motional narrowing limit formula. However, our analysis clearly shows that, in the presence of sizeable CEF splittings, τ is a complex quantity which contains a contribution from both quasielastic and inelastic excitations.

A more general expression for the damping rate λ_Z can be written in terms of the dynamical susceptibility:

$$\lambda_Z = \left[\sum_{\beta,\alpha} L_{\beta\alpha}(\theta,\varphi) M_{\alpha\beta}\right] \frac{1}{\chi_C}\lim_{\omega\to 0}\frac{\chi''[\omega]}{\omega}. \tag{18}$$

If the CEF effects are negligible, all of the multiplet energy levels are degenerate and $\chi''[\omega]/\omega$ can be taken as a quasielastic Lorentzian function with half-width at half-maximum Γ_Q. Then $\Gamma_{\mu\mathrm{SR}} = \Gamma_Q$.

In the general case, i.e. for a symmetry lower than cubic, λ_Z can be expressed as a linear combination of the spin–spin correlation functions of the paramagnet, as shown in section 2. Each of these functions can be computed according to the model developed above. This means that λ_Z can be written as a linear combination of terms such as that given by equation (15). Each of these terms refers to a specific correlation function, and the coefficients depend only on the muon site properties.

Equations (15) and (18) are written in terms of the Curie susceptibility. This does not presuppose that the compound susceptibility follows the Curie law. Our writing them in this way is just a practical method of obtaining compact equations.

3.2. Discussion

Formula (17) is similar to a well known nuclear magnetic resonance (NMR) formula which is often used to extract $1/\tau$ from $1/T_1$ data when the nuclear dynamics is dominated by the hyperfine coupling with the electronic spin. In common NMR practice, the possible effect of the inelastic excitations is usually neglected and $1/\tau$ is compared to the quasi-elastic linewidth measured by inelastic neutron scattering or is computed theoretically [15].

For rare-earth ions in the presence of CEF splittings, formula (17) has two drawbacks: the symmetry properties of λ_Z are not apparent and the physical meaning of τ is not explicit.

Concerning the first point, we have written the equations of section 2 in such a way that their symmetry properties are transparent. This is particularly important for μSR because the muon does not sit at the magnetic ion site. Therefore, as pointed out at the end of section 2, two types of spatial symmetry have to be considered: the symmetry of the spin–spin correlation functions, depending on the magnetic ion point symmetry group, and the symmetry at the muon site, which can be different from that of the magnetic ion site.

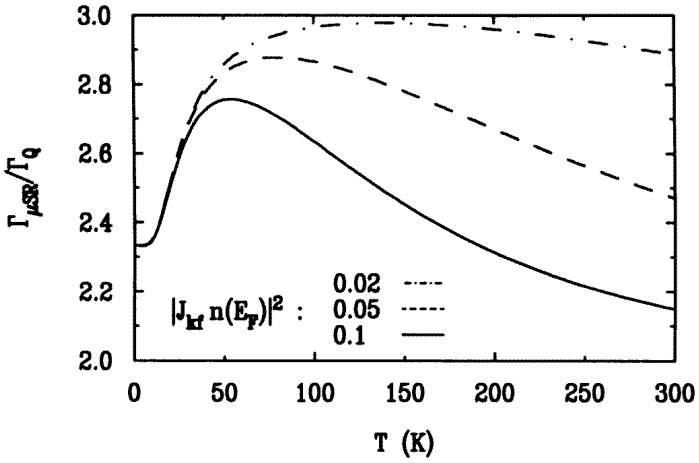

Figure 1. Thermal dependences of the ratio $\Gamma_{\mu\mathrm{SR}}/\Gamma_Q$ for the case of fluctuations driven by the 4f-conduction-electron exchange, for three values of the square of the 4f-conduction-electron coupling $|J_{kf}n(E_F)|^2$ (0.02, 0.05 and 0.1), in the presence of crystal-field splittings of the Yb^{3+} ion analogous to those in $YbAuCu_4$. $\Gamma_{\mu\mathrm{SR}}$ is probed in μSR experiments in zero or a weak longitudinal field, and Γ_Q is the quasi-elastic linewidth measured by neutron scattering.

As to the physical meaning of τ, we shall illustrate it through a model calculation of $\Gamma_{\mu\mathrm{SR}}$ and of the neutron quasi-elastic linewidth Γ_Q. We consider a Yb^{3+} ion sitting at a site with cubic symmetry in a metallic compound, and assume that its CEF level scheme is similar to that in $YbAuCu_4$ [16]: the Γ_7 doublet is the ground state, the Γ_8 quartet the first excited state at 3.9 meV (45 K) and the Γ_6 doublet lies at 6.9 meV (80 K) from the ground state. These CEF excitations are therefore of rather low energy, and when temperature grows, say, from 4.2 K to 300 K, one crosses from the regime $k_BT \ll E_m$ to the regime $k_BT \gg E_m$. We assume that the relaxation of the 4f moment $\boldsymbol{J}$ is solely due to its coupling with the conduction electron spin density through the classical kf exchange interaction [17]. Then, the dynamical linewidth for a transition from state $|m\rangle$ to state $|n\rangle$ is given by [18]

$$\Gamma_{mn}(T) = \frac{2\pi}{\hbar}(g_J - 1)^2\alpha^2 M_{mn}\frac{\Delta_{mn}}{\exp(\beta\Delta_{mn}) - 1} \tag{19}$$

where $\alpha = J_{kf}n(E_F)$ is the 4f-conduction-electron coupling constant, J_{kf} the kf exchange integral, $n(E_F)$ the electronic density of states at the Fermi level per spin direction and M_{mn} a matrix element for the transition from $|m\rangle$ to $|n\rangle$:

$$M_{mn} = 2|\langle m|J_z|n\rangle|^2 + |\langle m|J_+|n\rangle|^2 + |\langle m|J_-|n\rangle|^2. \tag{20}$$

When $m = n$, i.e. for a quasi-elastic line, the law (19) reduces to the classical Korringa law:

$$\Gamma_m = \frac{2\pi}{\hbar}(g_J - 1)^2 \alpha^2 M_{m\bar{m}} k_B T \tag{21}$$

where the state $|\bar{m}\rangle$ is the Kramers conjugate of $|m\rangle$. The quasi-elastic line as measured by inelastic neutron scattering corresponds to the first term of (8). Because it is a sum of various Lorentzian contributions with different widths, its shape is not exactly Lorentzian. One can however estimate Γ_Q with good precision by fitting the line with a Lorentzian. We have computed the thermal variation of the ratio $r(T) = \Gamma_{\mu\mathrm{SR}}/\Gamma_Q$ for three values of α^2. The result is shown in figure 1. At low temperature, the ratio tends towards

$$r(T=0) = \frac{J(J+1)}{3|\langle g|J_z|g\rangle|^2} \tag{22}$$

where $|g\rangle$ is the CEF doublet ground state (Γ_7 in our example). The thermal variation of $r(T)$ is non-monotonic, but $\Gamma_{\mu\mathrm{SR}}$ remains always larger than Γ_Q. At high temperature, the ratio $r(T)$ decreases as temperature increases, more rapidly with increasing α^2-values, i.e. with increasing dynamical widths. Our calculation shows that the asymptotic limit of $r(T)$ is close to 2, corresponding to the fact that at very high temperature, the quasi-elastic and inelastic lines merge together, the resulting line being roughly twice as broad as the quasi-elastic line.

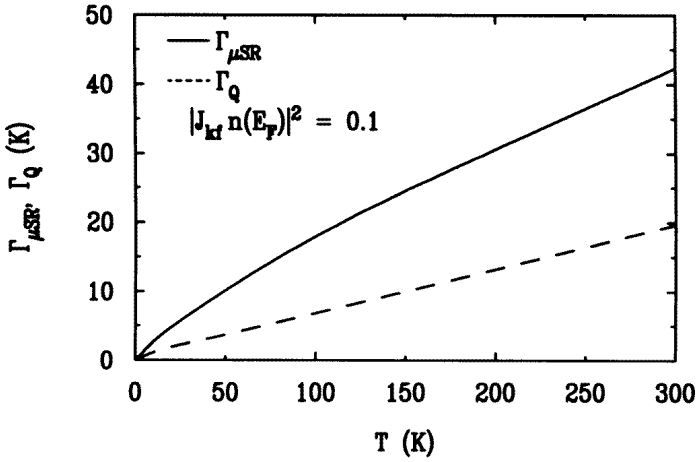

Figure 2. Thermal dependences of the dynamical linewidths $\Gamma_{\mu\mathrm{SR}}$ (full line) as probed by μSR and Γ_Q, the quasi-elastic neutron scattering linewidth (dashed line), in the presence of crystal-field splittings of the Yb^{3+} ion, for $|J_{kf}n(E_F)|^2 = 0.1$.

The thermal variation of $\Gamma_{\mu\mathrm{SR}}$ and of Γ_Q is shown in figure 2 for $\alpha^2 = 0.1$. Above 50 K, the quasi-elastic width shows a linear Korringa behaviour as expected; the initial slope is different, corresponding to the quasi-elastic width of the ground state alone. As to $\Gamma_{\mu\mathrm{SR}}(T)$, it shows a pronounced downward curvature below 150 K, and recovers a linear Korringa-type variation only at high temperature. This is due to the contribution of the inelastic linewidths which have a non-linear behaviour for $k_B T \sim \Delta_{mn}$ (expression (19)). It is to be emphasized that this model calculation does not apply in the actual case of $YbAuCu_4$ because of the presence of the Kondo coupling. The thermal variation of Γ_Q in

$YbAuCu_4$ shows a downward curvature [16], and that of $\Gamma_{\mu SR}$ is detailed in [2]. A tentative interpretation of these data within a Kondo model is given in [2].

4. Analysis of some published longitudinal relaxation rate data

In this section we present a preliminary analysis of published μSR relaxation rate data recorded for the strongly correlated electron systems CeNiSn and $CePt_2Sn_2$, where the Kondo coupling is expected to play a major role, using the theoretical framework that we have established. We first summarize the theoretical predictions concerning the relaxation rate of a 4f angular momentum in the presence of Kondo coupling.

4.1. The relaxation rate of a Kondo ion

The computation of the quasi-elastic relaxation rate Γ_Q for a Kondo ion with degeneracy N_f, both below and above the Kondo temperature T_0, has been achieved through the computation of the f excitation spectrum $P^{NCA}(\omega, T)$ using the $1/N_f$ expansion technique in the NCA scheme [12]. Although the excitation spectrum in the presence of hybridization is found to have a non-Lorentzian shape, especially for $T < T_0$, $\hbar\Gamma_Q(T)$ is identified with the energy for which the function $\hbar\omega P^{NCA}(\omega, T)$ goes through a maximum. For a Lorentzian-shaped $P(\omega, T)$, this coincides with the half-width. The quasi-elastic width Γ_Q is found to be of the order of $k_B T_0/\hbar$ for $T \ll T_0$, then it goes through a minimum for $T \simeq T_0$, and increases with further increase of the temperature according to the semi-empirical law, holding for $T \gtrsim 5T_0$,

$$\Gamma_Q(T) = \frac{2.4}{N_f}\frac{k_B T_0}{\hbar}\sqrt{\frac{T}{T_0}}. \tag{23}$$

The NCA calculation of [12] has been performed without taking account of the CEF splittings. The extension to the CEF case will be given in [2]. In this respect, it should be emphasized that the Kondo temperature is renormalized by the presence of the CEF splittings. The above-mentioned T_0 can be said to be a 'high-temperature Kondo scale', i.e. describing properties at a temperature much higher than the CEF splittings: $k_B T \gg E_m$. In order to describe the low-temperature Kondo properties, the energy scale $k_B T_K$ is relevant, related to $k_B T_0$ by the following expression, obtained through the variational solution of the Kondo problem at $T = 0$ K [19, 20]:

$$\prod_m \left(\frac{E_m}{k_B} + T_K\right) = (T_0)^{N_f}. \tag{24}$$

4.2. Preliminary analysis of CeNiSn and $CePt_2Si_2$ μSR data

The Kondo insulator CeNiSn has attracted much interest because it is believed that its energy gap is produced by the hybridization of the 4f electrons with the conduction electrons. No inelastic CEF structures have been observed in the neutron scattering spectra of this compound at high temperature; at low temperature, the remarkable result has been found that while the inelastic magnetic excitation is strongly dependent on the momentum transfer $\boldsymbol{Q}$, the zero-frequency response function is independent of $\boldsymbol{Q}$ [21]. Recently some μSR transverse-field relaxation data have been reported by Kalvius *et al* [22]. Although our theoretical analysis has only considered data recorded in zero field, we do not expect the temperature dependence of the zero-field and transverse-field relaxation rates to be much

different. The μSR data confirm that CeNiSn does not order magnetically, at least down to 11 mK. Interestingly, Kalvius *et al* observe that the μSR relaxation rate λ_Z is proportional to $1/\sqrt{T}$ for 0.1 K $\lesssim T \lesssim$ 2 K. At lower temperature it becomes temperature independent. The spectra have been recorded in a strong transverse field (0.1 T) and therefore could be influenced by inhomogeneities due to demagnetization-field effects. However, the measured $\sqrt{T}$-behaviour of $1/\lambda_Z$ seems to indicate that the Ce ions at low temperature behave as independent Kondo ions, consistently with the neutron results [21]. Following Cox *et al* [12], the temperature at which λ_Z becomes temperature independent is identified as the Kondo temperature. Therefore $T_K \simeq 0.1$ K for CeNiSn. One potential problem with our interpretation is that it supposes that the CEF effects are negligible. Up to now it does not seem that there is detailed information available on the CEF energy levels in CeNiSn. We note that recently it has been proposed that the most characteristic feature of a system like CeNiSn is the presence of low-lying CEF energy levels [23, 24]. If the CEF energy level splitting is as small as ∼0.1 K, then the work presented in this report fully justifies the observed $\sqrt{T}$-behaviour of $1/\lambda_Z$. Interestingly, whereas at very small energy transfer the Ce ions behave as isolated ions as indicated by the neutron analysis and our analysis of the μSR results, the inelastic neutron measurements show that the inelastic excitations are strongly influenced by the inter-site correlations [21].

The heavy-fermion compound $CePt_2Sn_2$ has recently attracted considerable attention because of its enormous linear specific heat coefficient ($\gamma > 3$ J mol^{-1} K^{-2}), consistent with its low Kondo temperature ($T_K \sim 1$ K). A μSR study by Luke *et al* [25] has shown that the dynamics evolves over a wide temperature range. From 200 K down to 20 mK, the depolarization function is found to be a generalized exponential, $P_Z(t) = \exp[-(\lambda_Z t)^\beta]$, with the exponent $\beta = 1$ above 0.7 K, while at low temperature β increases towards a value of 2. The results below 0.7 K have recently been disputed by Lidström [26]. This author argues that in fact the low-temperature spectra are best fitted with a damped oscillating signal characterized by a low frequency. This means that the compound orders magnetically at $T_N \sim 0.7$ K. Therefore we shall not discuss any longer the $\lambda_Z(T)$ results of [25] for $T < T_N$. In the paramagnetic state $\lambda_Z(T)$ decreases very slowly as temperature increases up to $T_* \sim 20$ K and then presents a sharp decrease (an order of magnitude) up to the highest measured temperature (200 K). Luke *et al* [25] identify T_* with the Kondo temperature. They note that it is considerably larger than the value determined from the neutron scattering data [27]. This is not surprising because the temperature at which $\lambda_Z(T)$ starts to change rapidly with temperature can be taken as the Kondo temperature only in the absence of CEF effects. In $CePt_2Sn_2$, the first excited CEF doublet seems to be located at 29 K [28]. Therefore we expect a strong CEF effect on the behaviour of $\lambda_Z(T)$ in this compound. Because of the strong temperature dependence of λ_Z for $T > T_*$, we infer that the lifetime of the inelastic excitations is remarkably short. But before giving a definite interpretation of the published μSR data, more μSR (measurements of $\lambda_Z(T)$ for different crystal orientations) and neutron data are needed. In particular, researchers should attempt to observe via inelastic neutron scattering the CEF transitions. Anyway, our analysis clearly shows that the Kondo temperature cannot be deduced from an inflection point in the temperature dependence of λ_Z, as had been done in [25].

5. Summary

We have analysed the meaning of the depolarization rate λ_Z measured in μSR experiments performed in zero or weak longitudinal fields, in the paramagnetic phase of compounds containing 4f-shell ions. The two main hypotheses of our calculation are the validity of the

'extreme narrowing' regime for the fluctuation frequency of the rare-earth ion with respect to its coupling to the muon spin, and the absence of inter-site correlations between rare-earth ions. This approach holds at high temperature, well above the magnetic transition temperature, and for fluctuation frequencies of the order of magnitude of 10 GHz or more. We treated the case where the CEF splittings of the rare-earth ion are sizeable (typically, in intermetallic compounds, they amount to a few 100 K). We have shown that the equivalent dynamical width $\Gamma_{\mu\mathrm{SR}}$ extracted from the λ_Z-value cannot be directly compared with the dynamical quasi-elastic width Γ_Q measured by neutron scattering. The expression that we derived for $\Gamma_{\mu\mathrm{SR}}$ shows that it contains contributions from both the quasi-elastic and inelastic excitations; even at low temperature the ratio $\Gamma_{\mu\mathrm{SR}}/\Gamma_Q$ is different from unity. For the case where the 4f fluctuations are driven by normal exchange with conduction electrons (i.e. no Kondo effect), we have shown that the thermal variation of $\Gamma_{\mu\mathrm{SR}}$ shows a marked $\sqrt{T}$-like curvature in the temperature range Δ_{mn}/k_B, where Δ_{mn} is a typical CEF splitting.

It should be noted that the μSR technique measures the fluctuations at zero energy transfer. For the analysis of the data, one does not need to suppose that the spectral functions are Lorentzian. This has been done in section 3.2 only for the purpose of comparing the μSR and neutron linewidths.

We have also given a short discussion concerning the measured thermal variation of the depolarization rate in two strongly correlated electronic systems, CeNiSn and $CePt_2Sn_2$, where the Kondo effect plays a major role.

We stress that μSR spin dynamics studies should be performed, at least as a first step, in zero field or weak longitudinal fields: it is easier to interpret longitudinal-field than transverse-field relaxation data, simply because the expression for the transverse relaxation rate in terms of the correlation functions is complicated [29]. Up to now there has been no detailed framework available for analysing transverse-field data. In addition the spectra recorded in transverse fields can be influenced by demagnetization effects.

In our analysis we do not address the question of possible perturbation of the crystal field by the electric muon charge, an effect which may have been seen recently [30]. The coupling between the muon spin and the 4f ion being short range, our framework is still valid provided that the μSR dynamical width is expressed in terms of the CEF level scheme which is modified by the muon charge.

Appendix A. Expressions for the $L(\theta, \varphi)$ matrix elements

The matrix elements which allow us to express the μSR relaxation rate in terms of the lattice-field correlation tensor are given in this appendix. $L(\theta, \varphi)$ is a symmetric matrix. We have

$$L_{xx} = \cos^2\varphi\cos^2\theta + \sin^2\varphi \tag{A1}$$

$$L_{yy} = \sin^2\varphi\cos^2\theta + \cos^2\varphi \tag{A2}$$

$$L_{zz} = \sin^2\theta \tag{A3}$$

$$L_{xy} = -\cos\varphi\sin\varphi\sin^2\theta \tag{A4}$$

$$L_{xz} = -\cos\varphi\cos\theta\sin\theta \tag{A5}$$

$$L_{yz} = -\sin\varphi\cos\theta\sin\theta. \tag{A6}$$

For the analysis of data taken on a polycrystalline sample it is useful to have the spherical average of the matrix elements. The average of each diagonal element is $2/3$. The average of each of the non-diagonal elements is zero.

References

[1] Amato A 1994 *Physica* B **206+207** 49
[2] Bonville P, Dalmas de Réotier P, Yaouanc A, Polatsek G, Gubbens P C M and Mulders A M 1996 *J. Phys.: Condens. Matter* at press
[3] Chappert J and Grynszpan R I (ed) 1984 *Muons and Pions in Materials Research* (Amsterdam: North-Holland)
[4] Karlsson E B 1995 *Solid State Phenomena as seen by Muons, Protons and Excited Nuclei* (Oxford: Clarendon)
[5] Yaouanc A, Dalmas de Réotier P, Gubbens P C M, Kayzel F, Bonville P, Franse J J M and Mulders A M 1995 *J. Magn. Magn. Mater.* **140–144** 1949
[6] Yaouanc A, Dalmas de Réotier P and Frey E 1993 *Europhys. Lett.* **21** 93; 1993 *Phys. Rev.* B **47** 796
[7] Dalmas de Réotier P and Yaouanc A 1994 *Phys. Rev. Lett.* **72** 290
[8] Lovesey S W 1987 *Theory of Neutron Scattering From Condensed Matter* vol 2 (Oxford: Clarendon)
[9] Becker K W, Fulde P and Keller J 1977 *Z. Phys.* B **28** 9
[10] Richards P M 1984 *Magnetic Excitations and Fluctuations* ed S W Lovesey, U Balucani, F Borsa and V Tognetti (Berlin: Springer)
[11] Maleyev S V 1994 *Phys. Rev.* B **50** 302
[12] Cox D L, Bickers N E and Wilkins J W 1985 *J. Appl. Phys.* **57** 3166
[13] Maekawa S, Takahashi S, Kashiba S and Tachiki M 1985 *J. Phys. Soc. Japan* **54** 1955
[14] Holland-Moritz E, Wohlleben D and Loewenhaupt M 1982 *Phys. Rev.* B **25** 7482
[15] See, for example,
Benakki M, Kappler J P and Panissod P 1987 *J. Phys. Soc. Japan* **56** 3309
[16] Severing A, Murani A P, Thompson J D, Fisk Z and Loong C-K 1990 *Phys. Rev.* B **41** 1739
[17] Kasuya T 1956 *Progr. Theor. Phys.* **16** 45
[18] Hirst L L 1977 *Phys. Rev.* B **15** 1
[19] Gunnarsson O and Schönhammer K 1983 *Phys. Rev.* B **28** 4315
[20] LeBras G 1994 *Thesis* Orsay–Paris XI University
[21] Mason T E, Aeppli G, Ramirez A P, Clausen K N, Broholm C, Stücheli N, Bucher E and Palstra T T M 1992 *Phys. Rev. Lett.* **69** 490
[22] Kalvius G M, Kratzer A, Wäppling R, Takabatake T, Nakamoto G, Fujii H, Kiefl R F and Kreitzmann S R 1995 *Physica* B **206+207** 807
[23] Kagan Yu, Kikoin K A and Prokof'ev N V 1993 *Pis. Zh. Eksp. Teor. Fiz.* **57** 584 (Engl. Transl. *JETP Lett.* **57** 600)
[24] Kagan Yu and Kalvius G M 1995 *Pis. Zh. Eksp. Teor. Fiz.* **61** 743 (Engl. Transl. *JETP Lett.* **61** 758)
[25] Luke G M, Keren A, Kojima K, Le L P, Wu W D, Uemura Y J, Kalvius G M, Kratzer A, Nakamoto G, Takabatake T and Ishikawa M, 1995 *Physica* B **206+207** 222
[26] Lidström E 1995 *Dissertation* Acta Universitatis Upsaliensis, Uppsala
[27] Mignot J-M, Kahn R, Besnus M-J, Kappler J-P and Godart C 1993 *Physica* B **186–188** 475
[28] Shigeoka T, Hirota H, Ishikawa M, Takabatake T and Fujii H 1993 *Physica* B **186–188** 469
[29] Dalmas de Réotier P and Yaouanc A 1992 *J. Phys.: Condens. Matter* **4** 4533
[30] Feyerherm R, Amato A, Grayevsky A, Gygax F N, Kaplan N and Schenck A 1995 *Z. Phys.* B **99** 3